ARL-TR-8821 • Sep 2019

DEVCOM ARMY RESEARCH LABORATORY

Optimization of Heat Transfer with Application to Gun Barrel Design

by David A Hopkins and
Raymond A Wildman

NOTICES

Disclaimers

The findings in this report are not to be construed as an official Department of the Army position unless so designated by other authorized documents.

Citation of manufacturer's or trade names does not constitute an official endorsement or approval of the use thereof.

Destroy this report when it is no longer needed. Do not return it to the originator.

ARL-TR-8821 ● SEP 2019

Optimization of Heat Transfer with Application to Gun Barrel Design

by David A Hopkins
Raymond A Wildman
Weapons and Materials Research Directorate, CCDC Army Research Laboratory

REPORT DOCUMENTATION PAGE

Form Approved
OMB No. 0704-0188

PLEASE DO NOT RETURN YOUR FORM TO THE ABOVE ADDRESS.

1. REPORT DATE *(DD-MM-YYYY)*	2. REPORT TYPE	3. DATES COVERED (From - To)
September 2019	Technical Report	January 2018 – August 2018

4. TITLE AND SUBTITLE
Optimization of Heat Transfer with Application to Gun Barrel Design

5a. CONTRACT NUMBER

5b. GRANT NUMBER

5c. PROGRAM ELEMENT NUMBER

6. AUTHOR(S)
David A Hopkins and Raymond A Wildman

5d. PROJECT NUMBER
AH80

5e. TASK NUMBER

5f. WORK UNIT NUMBER

7. PERFORMING ORGANIZATION NAME(S) AND ADDRESS(ES)
CCDC Army Research Laboratory
ATTN: FCDD-RLW-MB
Aberdeen Proving Ground, MD 21005-5066

8. PERFORMING ORGANIZATION REPORT NUMBER
ARL-TR-8821

9. SPONSORING/MONITORING AGENCY NAME(S) AND ADDRESS(ES)

10. SPONSOR/MONITOR'S ACRONYM(S)

11. SPONSOR/MONITOR'S REPORT NUMBER(S)

12. DISTRIBUTION/AVAILABILITY STATEMENT
Approved for public release; distribution is unlimited.

13. SUPPLEMENTARY NOTES
primary author's email: <david.a.hopkins.civ@mail.mil>.

14. ABSTRACT
Additive manufacturing provides an opportunity to realize gun tube designs that are not normally considered. Optimization techniques to determine the possible advantages of finned gun tubes over existing tube designs were examined. Two methods were implemented to explore the effect of gun tube geometry on thermal and mechanical performance. One method used a boundary integral approach. The other used a parametric fin design with a finite element method. It is shown that the long-term maximum temperature in a barrel can be reduced by the addition of fins. However, without increased external convection, this advantage is of minimal consequence as the overall temperature rise is still unacceptable.

15. SUBJECT TERMS
additive manufacturing, optimization, heat transfer, gun tubes

16. SECURITY CLASSIFICATION OF:			17. LIMITATION OF ABSTRACT	18. NUMBER OF PAGES	19a. NAME OF RESPONSIBLE PERSON
a. REPORT	b. ABSTRACT	c. THIS PAGE			David A Hopkins
Unclassified	Unclassified	Unclassified	UU	31	19b. TELEPHONE NUMBER (Include area code) 410-306-0764

Contents

List of Figures

List of Tables

1. Introduction

Additive manufacturing's (AM) capability to provide on-site fabrication of gun components is enticing. AM also provides an opportunity to reconsider how gun barrels could be designed using more complex geometries that are difficult to fabricate by traditional casting and forging. However, the AM process can result in material properties that do not have the strength and thermal properties of high-strength gun steel due to the introduction of defects during the manufacturing process.[1] Optimization techniques can be employed to mitigate these possible issues. In this report, we first review the fundamental structural requirements of a gun tube. Next, we briefly discuss optimization techniques and how they can be applied in the context of designing a barrel. Specifically, two geometry parameterization and solution techniques are described, each having relative strengths and weaknesses. The first is a Fourier-like expansion of the radial coordinate of the external gun tube cross section, coupled with boundary integral solution methods. The second is a parameterized fin design in which the number of fins and fin geometry (thickness and height) are the optimization parameters. A transient thermal model is used for the analysis of these designs. Results of these techniques are given and discussed in context of practical design considerations.

2. Review of Gun Barrel Design

While the details of gun tube design can be complex, a gun tube is, in essence, simply a pressure vessel.[2] The goal of the design, then, is likewise straightforward: given the design specifications, such as maximum internal pressure, maximum temperature, and desired exit velocity of a projectile, select the appropriate materials and tube geometry that meet these requirements. While the internal pressure is the dominant effect, other effects such as temperature, gun tube wear, dynamic strain,[3,4] and gun tube/projectile interaction are also important. These effects have been studied extensively by numerous researchers.[5–8]

Lamés quasi-static equations for a pressurized cylinder provide the starting point for determining the wall thickness required to withstand a given internal pressure. In fact, for projectile velocities below the critical axial wave velocity, these equations are completely sufficient for the initial design as dynamic strain effects can be neglected.[3]

Accordingly, the tangential (circumferential) stress is given by[2,9]

$$\sigma_t(D) = \frac{D_i^2(D_o^2 + D^2)}{D^2(D_o^2 - D_i^2)}p, \tag{1}$$

where D_i is the inside diameter, D_o is the outside diameter, D is the diameter at which the stress is to be found, and p is the internal pressure.

The radial stress is given by

$$\sigma_r(D) = -\frac{D_i^2(D_o^2 - D^2)}{D^2(D_o^2 - D_i^2)}p. \tag{2}$$

Equations 1 and 2 are valid for an isotropic, elastic material. Inclusion of temperature dependencies and anisotropic material properties complicate the equations. While some analytic solutions to the temperature-dependent, anisotropic equations can be found with suitable simplifying assumptions, computational techniques are more often used.[10–13] Prediction of the actual performance of a gun tube also necessitates consideration of the 3-D response of the gun system.[14] However, in the present study, we are only concerned with determining the structural response at a single cross section of the tube subjected to a transient temperature.

The maximum temperature to which the barrel is subjected is the gas temperature of the propellant. To determine the gun tube temperature profile due to a single shot requires a gas temperature-time curve and a corresponding heat transfer coefficient versus time curve, where the heat transfer coefficient may be temperature-dependent. The XKTC interior ballistics code[15,16] was used to obtain these curves. A typical gas temperature-time curve near the breech is shown in Fig. 1. The results from XKTC are in general agreement with experimentally obtained results.[17] XKTC was also used to determine the heat transfer coefficient at axial locations along the bore. Figure 2 displays a typical heat transfer coefficient versus time relationship for a typical barrel.

For a single shot, the temperature rise in the barrel, while significant, is not necessarily detrimental.[5] However, for repeated firing, the temperature in the barrel can exceed the anneal temperature, and possibly the melt temperature, of the barrel material.[2] To simulate repeated firing, the single-shot curves were extended by cycling the single-shot temperature and heat coefficient curves at the firing rate.

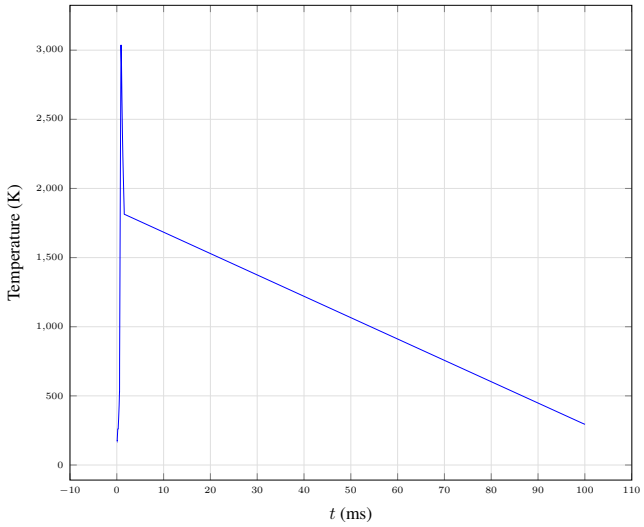

Fig. 1. Temperature time history at breech

This approximation to the actual repeated firing curves provides a lower bound on the expected temperature profiles, and thus, a best-case scenario for any potential design.

3. Shape Optimization approach

The optimization of the gun barrel shape is perhaps not actually a topology optimization problem as the decision to use fins to aid in cooling the barrel is made a priori, which consequently reduces the optimization process to determining the optimum fin geometry. However, with that in mind, we review the basic approach that can be taken if a more generic shape optimization approach is used. As stated earlier, the gun tube must withstand the internal pressure and dissipate heat at a sufficient rate to keep the maximum temperature below acceptable levels. Additionally, though not part of the optimization process, we can anticipate that natural convection may not be sufficient to meet the temperature requirement. Therefore, forced convection can also be assumed and included by an assumed value for the external convective heat transfer coefficient with the details of a design to implement forced convection left unspecified. To minimize the number of unknowns, the optimization problem can be formulated using integral equations, in particular, boundary integral equations. This means that only the boundary geometry is required. It can be additionally assumed that the external boundary can be represented by a Fourier expansion in the radial direction, and that the exterior boundary shape is periodic in

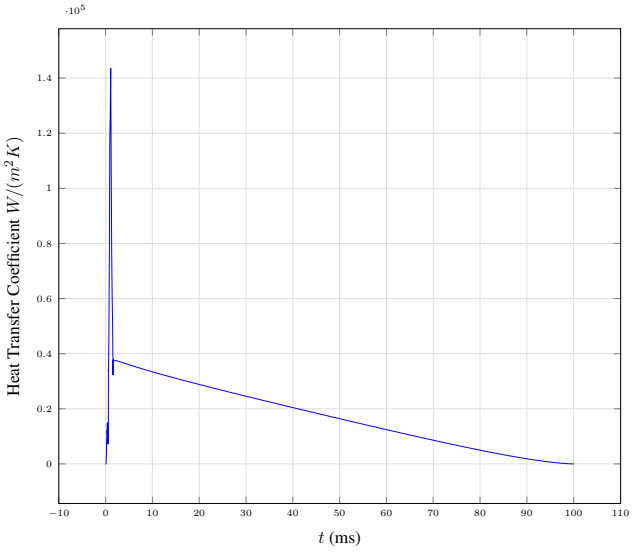

Fig. 2. Convective heat transfer coefficient at breech

the circumferential direction.

Consider the generic shape shown in Fig. 3. The optimization problem can then be stated as

$$\begin{aligned} &\min_{\Gamma} f(\Gamma) = wc(\Gamma) + (1-w)\, T_{\text{int}}(\Gamma) \\ &\text{subject to } V(\Gamma) < V_0, \end{aligned} \tag{3}$$

where Γ is parameterized in polar coordinates as

$$r(\theta) = \sum_{i=1}^{N} c_i \cos(f_i \theta), \tag{4}$$

where $c(\Gamma)$ is the compliance, w is the weighting factor, and V_0 is the maximum allowable volume of material. The parameters c_i, f_i, and N collectively define the amplitude, cyclic frequency, and total number of terms allowed for the fins optimization, respectively. The internal temperature T_{int} is the maximum temperature on the boundary,

$$T_{\text{int}} = \max T(\mathbf{r})\,|_{\mathbf{r}\in\Gamma_N}\,. \tag{5}$$

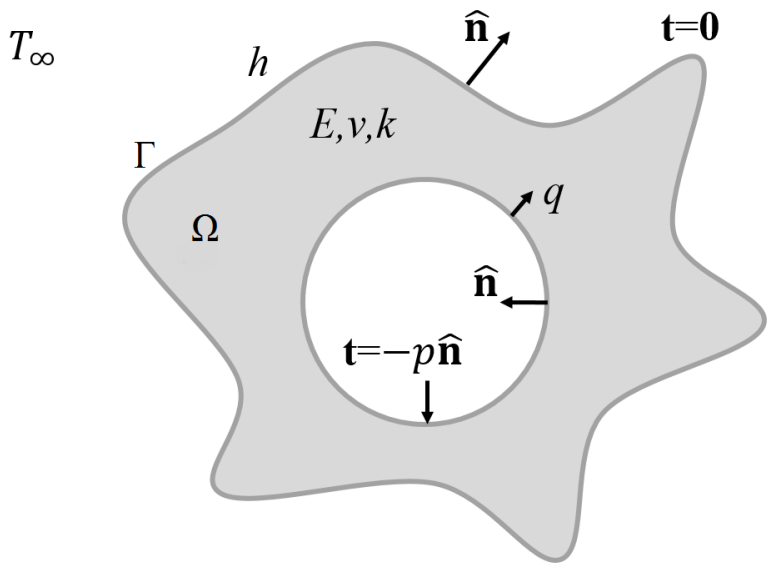

Fig. 3. Generic shape

3.1 Problem Formulation

We now turn to the development of the boundary integral equations, which may be used for both the thermal and mechanical analysis of the gun barrel designs.

The boundary integral equation formulation is straightforward. All that is required is an appropriate Green's function for the desired physics, an integral identity, and specification of the boundary conditions. In the following, we restrict ourselves to considering a 2-D thermomechanical response of a structure, which represents the cross section of the gun barrel. For the structural response, we assume the barrel is in a state of plane strain. Accordingly, Kelvin's fundamental solution for the displacement due to a unit point force in an infinite homogeneous medium is given by

$$u_j(\mathbf{r}) = U_{ij}(\mathbf{r}, \mathbf{r}')e_i(\mathbf{r}'), \tag{6}$$

where $e_i(\mathbf{r})$ is a unit load in the $\hat{\mathbf{i}}$ direction,

$$U_{ij}(\mathbf{r}, \mathbf{r}') = \frac{-1}{8\pi G\,(1-\nu)}\left[(3-4\nu)\,\delta_{ij}\log R - \nabla R\cdot\hat{\mathbf{i}}\nabla R\cdot\hat{\mathbf{j}}\right], \tag{7}$$

where $R = |\mathbf{r}-\mathbf{r}'|$, G is shear modulus, δ_{ij} is the Kronecker delta, and ν is Poisson's ratio.

The tractions due to the unit point force are given by

$$t_j(\mathbf{r}) = T_{ij}(\mathbf{r}, \mathbf{r}')e_i(\mathbf{r}'), \tag{8}$$

where

$$\begin{aligned} T_{ij}(\mathbf{r}, \mathbf{r}') = \frac{-1}{4\pi\,(1-\nu)\,R} \{&(1-2\nu)\,(\hat{\mathbf{n}} \times \nabla R) \cdot \hat{\mathbf{z}}\,(1-\delta_{ij}) \\ &+ \left[2\nabla R \cdot \hat{\mathbf{i}} \nabla R \cdot \hat{\mathbf{j}} + (1-2\nu)\,\delta_{ij}\right] \hat{\mathbf{n}} \cdot \nabla R \Big\}. \end{aligned} \tag{9}$$

Equations 7 and 9 are the required Green's functions. We derive the integral identity from Betti's reciprocal work theorem.[18] Specifically, Betti's work theorem is given by

$$\begin{aligned} \int_\Gamma t_j^*(\mathbf{r}) u_j(\mathbf{r}) d\mathbf{r} + \int_\Omega b_j^*(\mathbf{r}) u_j(\mathbf{r}) d\mathbf{r} \\ = \int_\Gamma t_j(\mathbf{r}) u_j^*(\mathbf{r}) d\mathbf{r} + \int_\Omega b_j(\mathbf{r}) u_j^*(\mathbf{r}) d\mathbf{r}. \end{aligned} \tag{10}$$

Betti's theorem is often used in the design of compliant mechanisms by a topology optimization approach.[19] Substituting the expression for the unit test forces, Eqs. 7 and 8, and assuming no body forces results in

$$u_j(\mathbf{r}') = \int_\Gamma U_{ij}(\mathbf{r}, \mathbf{r}') t_j(\mathbf{r}) d\mathbf{r} - \int_\Gamma T_{ij}(\mathbf{r}, \mathbf{r}') u_j(\mathbf{r}) d\mathbf{r}. \tag{11}$$

Equation 11 is only valid for determining the displacement $u_j(\mathbf{r}')$ in the interior of the body, that is the domain Ω, but not on the boundary Γ. By determining the limit as a point approaches the boundary Γ, we obtain the final form in terms of the boundary as

$$\frac{1}{2}\delta_{ij} u_j(\mathbf{r}') = \int_\Gamma U_{ij}(\mathbf{r}, \mathbf{r}') t_j(\mathbf{r}) d\mathbf{r} - \text{p.v.} \int_\Gamma T_{ij}(\mathbf{r}, \mathbf{r}') u_j(\mathbf{r}) d\mathbf{r}, \tag{12}$$

where p.v. means principal value. The final required ingredient is the specification of displacement and traction boundary conditions. For a well-posed problem, we can specify either of these on different parts of the boundary, but we cannot specify both on the same section of the boundary. That is, if Γ_u is the section of the boundary with a displacement boundary condition specified, and Γ_t is the boundary where a

traction boundary condition is specified, then

$$\Gamma_u \cup \Gamma_t = \Gamma$$
$$\Gamma_u \cap \Gamma_t = \emptyset.$$

With these boundary conditions, Eq. 12 becomes

$$\begin{aligned}\frac{1}{2}\delta_{ij}u_j(\mathbf{r}') - \int_{\Gamma_u} U_{ij}(\mathbf{r},\mathbf{r}')t_j(\mathbf{r})d\mathbf{r} + \text{p.v.}\int_{\Gamma_t} T_{ij}(\mathbf{r},\mathbf{r}')u_j(\mathbf{r})d\mathbf{r} \\ = \int_{\Gamma_t} U_{ij}(\mathbf{r},\mathbf{r}')t_j^{bc}(\mathbf{r})d\mathbf{r} - \text{p.v.}\int_{\Gamma_u} T_{ij}(\mathbf{r},\mathbf{r}')u_j^{bc}(\mathbf{r})d\mathbf{r},\end{aligned} \tag{13}$$

where t_j^{bc} represents the specified boundary tractions and u_j^{bc} represents the specified boundary displacements.

Similarly, we can obtain the boundary integral formulation of the heat transfer equation. We also make a further simplifying assumption that the system is at steady state. We further assume there are no volumetric heat sources. Consequently, the governing equation is just the Laplace equation

$$\nabla^2 T = 0, \tag{14}$$

where T is temperature. The Green's function solution for the Laplace equation in 2-D is therefore

$$G(\mathbf{r},\mathbf{r}') = \frac{1}{2\pi}\log R. \tag{15}$$

To impose a convective heat transfer boundary condition, we require the gradient normal to the surface. This is given by

$$\hat{\mathbf{n}}\cdot\nabla G(\mathbf{r},\mathbf{r}') = -\frac{\hat{\mathbf{n}}\cdot(\mathbf{r}-\mathbf{r}')}{2\pi R^2}. \tag{16}$$

The boundary conditions are then given by internal heat flux

$$\hat{\mathbf{n}}\cdot\nabla T = -\frac{q}{k}, \tag{17}$$

and, as implied, external convection

$$\hat{\mathbf{n}}\cdot\nabla T = \frac{h}{k}\left(T_\infty - T\right), \tag{18}$$

where q is heat flux, k is conductivity, h is heat transfer coefficient, and T_∞ is ambient temperature. Finally, we can again use Betti's reciprocal theorem to obtain

$$\frac{1}{2}T(\mathbf{r}) = \text{p.v.} \int_\Gamma T(\mathbf{r}')\hat{\mathbf{n}}' \cdot \nabla' G(\mathbf{r}, \mathbf{r}')d\mathbf{r}' - \int_\Gamma \hat{\mathbf{n}}' \cdot \nabla' T(\mathbf{r}')G(\mathbf{r}, \mathbf{r}')d\mathbf{r}', \tag{19}$$

where $\hat{\mathbf{n}}'$ indicates the surface normal at the primed coordinate ($\mathbf{r}'$) and ∇' indicates differentiation with respected to the primed coordinate.

Equation 19 provides a relationship between the temperature and heat flux over the entire boundary. Thus, we still need to apply appropriate boundary conditions. As with the structural formulation, we have two boundary regions. On Γ_N, we have heat flux boundary conditions, while on Γ_R we impose convection boundary conditions. To simplify the exposition, we assume one or the other over the entire boundary. If we have both, it is then only necessary to integrate over the appropriate boundary as needed. Thus, assuming a flux boundary condition, Eq. 17, we obtain

$$\frac{q}{k}\int_\Gamma G(\mathbf{r}, \mathbf{r}')d\mathbf{r}' = \frac{1}{2}T(\mathbf{r}) - \text{p.v.} \int_\Gamma T(\mathbf{r}')\hat{\mathbf{n}}' \cdot \nabla' G(\mathbf{r}, \mathbf{r}')d\mathbf{r}'. \tag{20}$$

Similarly, assuming a convection boundary condition, Eq. 18 leads to

$$\begin{aligned} \frac{h}{k}T_\infty \int_\Gamma G(\mathbf{r}, \mathbf{r}')d\mathbf{r}' = &-\frac{1}{2}T(\mathbf{r}) \\ &+ \text{p.v.} \int_\Gamma T(\mathbf{r}') \left(\frac{h}{k}G(\mathbf{r}, \mathbf{r}') + \hat{\mathbf{n}}' \cdot \nabla' G(\mathbf{r}, \mathbf{r}') \right) d\mathbf{r}'. \end{aligned} \tag{21}$$

We can combine this equation with Eq. 20 to obtain the solution when both types of thermal boundary conditions are present.

Having determined the appropriate boundary integral equations, we can now return to the question of solving the optimization problem, Eq. 3. In particular, we are now able to specify the compliance as

$$c = \int_\Gamma \mathbf{u}(\mathbf{r}) \cdot \mathbf{t}(\mathbf{r})d\mathbf{r}. \tag{22}$$

3.2 Discretization

The integral equations developed have the general form

$$\phi(\mathbf{r}) = \int_{\Gamma} \psi(\mathbf{r}')g(\mathbf{r}, \mathbf{r}')d\mathbf{r}', \tag{23}$$

where $g(\mathbf{r}, \mathbf{r}')$ is the Green's function and ψ represents the unknown quantity, which can be discretized directly with an integration rule,

$$\phi(\mathbf{r}) = \sum_{n=1}^{N} \omega_n \psi(\mathbf{r}_n)g(\mathbf{r}, \mathbf{r}_n), \tag{24}$$

where the ω_n are integration weights and the $\mathbf{r}_n$ are the integration nodes on Γ. Typically, the contour Γ is divided into a set of curves, either as straight line segments or curved patches, and a Gaussian integration rule is applied on each individual curve. Further, by enforcing the equation at each integration point, an $N \times N$ system of equations in the form

$$\phi(\mathbf{r}_m) = \sum_{n=1}^{N} \omega_n \psi(\mathbf{r}_n)g(\mathbf{r}_m, \mathbf{r}_n), \tag{25}$$

where $m = 1, \ldots, N$ is obtained. The only remaining difficulty is that the integral equations to be solved are singular because of the Green's functions, thus making the evaluation of the matrix entries difficult. Specifically, the diagonal entries cannot be directly computed because of the singularity in the Green's function. Additionally, the near-diagonal entries will not be accurately integrated by the underlying integration rule because the Green's function near its singular point is not well approximated by polynomials. This is a known issue and there are several approaches to mitigating this issue and here we use the locally corrected Nyström method.[20]

The locally corrected Nyström method replaces the undefined and inaccurate matrix entries with a locally corrected kernel L_{mn}, with the discretized Green's function now defined as,

$$g(\mathbf{r}_m, \mathbf{r}_n) = \begin{cases} L_{mn} & \mathbf{r}_n \in D_m \\ g(\mathbf{r}_m, \mathbf{r}_n) & \text{otherwise}, \end{cases} \tag{26}$$

where D_m is the local correction domain, which is typically large enough to encompass a few near-by patches. The locally corrected kernel L_{mn} is then computed

so that it accurately integrates a family of polynomials f_k, which are typically Legendre polynomials,

$$\sum_{n=1}^{N} \omega_n L_{mn} f_k(\mathbf{r} - \mathbf{r}') = \int_{D_m} f_k(\mathbf{r}_m - \mathbf{r}') g(\mathbf{r}_m, \mathbf{r}') d\mathbf{r}'. \tag{27}$$

In order for L_{mn} to be accurate, the evaluation of the integrals on the right-hand side of Eq. 27 must be accurate and so their computation is accomplished by carefully considering the special cases that arise. For the problem formulation considered here, the singular integrals will involve polynomials, logarithmic singularities, and principal value terms of the form $1/x$. Assuming that the test functions are Legendre polynomials, each of these cases is reducible to one of the following forms to facilitate evaluation

$$\int_{-1}^{1} P_n(t) \log |x_m - t| \, dt = \frac{2}{2n+1} \left[Q_{n+1}(x_m) - Q_{n-1}(x_m) \right] \tag{28}$$

$$\text{p.v.} \int_{-1}^{1} \frac{P_n(t)}{x_m - t} dt \approx P_n(x_m) \left(\text{p.v.} \int_{-1}^{1} \frac{1}{x_m - t} dt \right) + \sum_{j=1}^{M} \omega_j \frac{P_n(t_j) - P_n(x_m)}{x_m - t_j} \tag{29}$$

$$\text{p.v.} \int_{-1}^{1} \frac{1}{x_m - t} dt = x_m \left[\log(x_m + 1) - \log(x_m - 1) \right] + \log(1 - x_m) + \log(t + 1) - 2, \tag{30}$$

where P_n is the n^{th} Legendre polynomial and Q_n is the n^{th} Legendre function of the second kind. The evaluation of the principal value integral in Eq. 29 involves separating it into singular and regular parts. The singular part is evaluated as given in Eq. 30 and the regular part is evaluated using a high-order Gaussian integration rule as expressed in Eq. 29. Each integral required to compute the locally corrected kernel entries L_{mn} may then be converted to a form that exposes its singularity type and evaluated using Eq. 28 and Eq. 30.

As a proof of concept for this approach, several test problems were evaluated.

3.3 Validation Test Cases

The first case considered is the elastic response of a thick-walled cylinder as shown in Fig. 4, where the inner radius is $r_i = 20$ mm, outer radius is $r_o = 30$ mm, internal pressure is $p = 100$ MPa, the shear modulus was $G = 209$ GPa, and Poisson's ratio was $\nu = 0.25$. For the discretization, the inner and outer boundaries were was divided into 40 and 60 straight line segments, respectively, and the underlying integration rule was Gaussian of order $N = 3$. The exact solution for the displacement is given by Timoshenko,[9]

$$u_r(r) = \frac{pr_i^2\,(1+\nu)}{E\,(r_o^2 - r_i^2)}\left[r\,(1-2\nu) + \frac{r_o^2}{r}\right]. \tag{31}$$

The numerical solution for the displacement, u are shown Fig. 5a where the initial

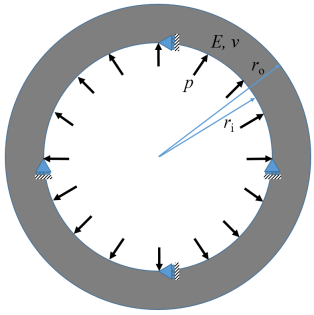

Fig. 4. Internally pressurized cylinder

geometry is shown blue and the scaled deformed geometry in red. The scale factor for the deformation was chosen to simply illustrate that the cylinder deformation was reasonable. Figure 5b shows a comparison between exact and Nyström solutions for this sample problem. The agreement between the exact solution and the Nyström numerical method is very good.

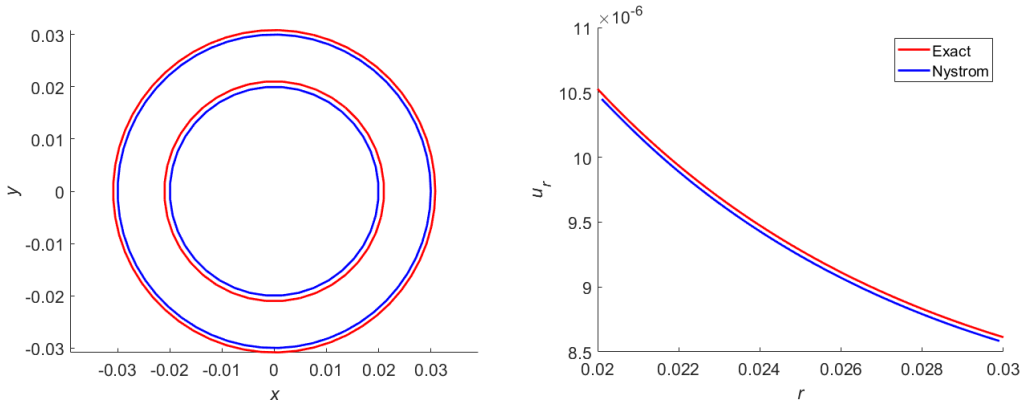

(a) Deformation of cylinder **(b) u_r [mm] within the cylinder**

Fig. 5. Displacement comparison

Next, the thermal heat conduction problem for a thick-walled cylinder was considered as shown in Fig. 6. where the inner radius r_i and outer radius r_o are the same as for the elastic case, internal heat flux is $q = 40$ kW/m^2, external transfer coefficient is $h = 4$ kW/m^{2}K, and the ambient temperature $T_\infty = 100$ K. The thermal conductivity for this example was $k = 40$ W/mK. The exact solution for this problem is given by[21]

$$T(r) = T_\infty + r_i q \left(\frac{1}{h r_o} + \frac{1}{k} \log r_o - \frac{1}{k} \log r \right), \tag{32}$$

The discretization is the same as for the elastic stress example. The numerical solution for the temperature at the inner and outer surface is shown in Fig. 7a. Figure 7b compares the exact solution with the numerical solution for the temperature profile through the thickness. Again, the agreement is excellent.

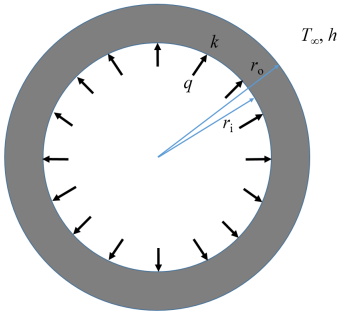

Fig. 6. Heat conduction thick-walled cylinder

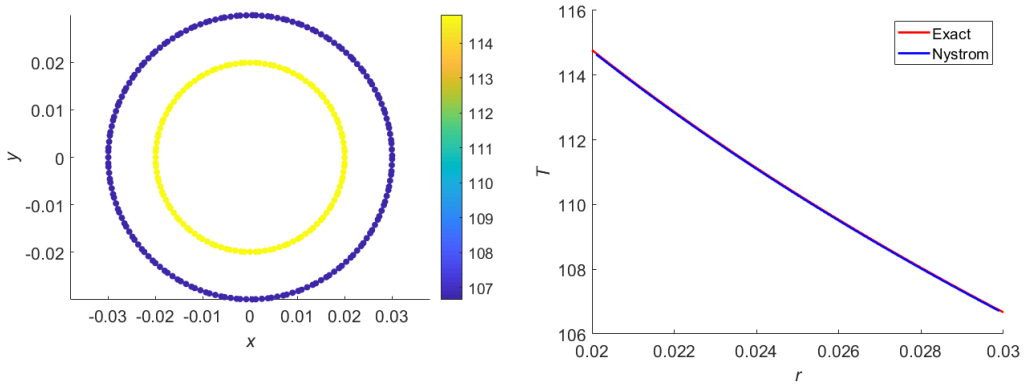

(a) Surface temperature T [K] on boundary of cylinder

(b) T [K] within the cylinder

Fig. 7. Temperature comparison

3.4 Gun Barrel Parameterization

Having verified the boundary integral formulations for the displacement and temperature, the next step is to couple these equations with an optimization scheme to examine optimization of the steady-state heat transfer in a pressurized cylinder. We assume that the exterior boundary of the gun barrel is parametrized in polar coordinates as

$$r(\theta) = \sum_{i=1}^{N} c_i \cos(f_i \theta), \tag{33}$$

where the circumferential frequency parameter f_i may be either specified or determine via optimization. In either case, it makes sense to specify $f_1 = 0$ so that a circular cylinder is included in the solution space. As an example of the utility of the optimization approach, two test cases were evaluated. For these test cases, the f_i and c_i were specified as shown in Table 1. The inner radius r_i was defined to be 0.2 m. Table 1 also shows the maximum temperature and the volume of the resultant unit length tube section. As these cases are simply a test of the approach, they do not use representative values for the inner or outer radius. The values for the heat flux and boundary temperatures are set for convenience. Figure 8a and 8b shows two geometries which are generated by Eq. 33. Thermal analysis of these shows that the geometry with more fins results in a slightly lower maximum temperature as seen in Table 1.

Table 1. Barrel shape optimization parameters and results

Case	Parameter	$i = 1$	$i = 2$	$i = 3$	$i = 4$	Temperature (K)	Volume (m^3)
Case 1	c_i	1	0.3	0.13	0.1	383	3.183
	f_i	0	10	20	30		
Case 2	c_i	1	0.3	0.13	0.1	358	3.185
	f_i	0	10	20	30		

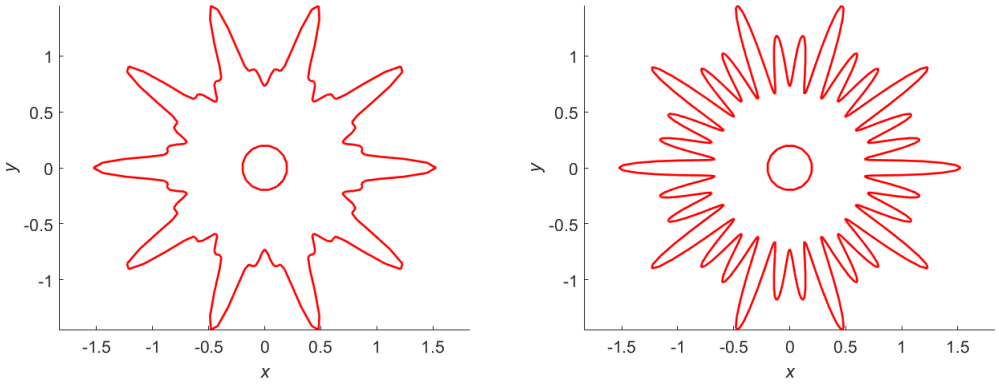

(a) Barrel Shape Case 1 **(b) Barrel Shape Case 2**

Fig. 8. Barrel shape test cases

Although we've shown it is possible to formulate the steady-state thermomechanical optimization problem using a boundary integral approach, there are several issues that render use of such an approach untenable in general. First, the formulation presented is strictly limited to steady-state response. This enforces a time-invariant condition on the temperature and heat flux bouundary conditions. An actual gun temperature-time history has significant variance, as shown earlier. To accommodate multiple shots, the steady-state assumption cannot be assumed up front. Instead, it is necessary to reach steady state via a transient analysis. However, optimization problems are not well suited for addressing the optimization of transient loading though some work has been done in this area.[22,23] Second, the formulation just presented is an uncoupled analysis in the sense that material properties and the heat transfer coefficient are not temperature-dependent. Finally, the analysis also does not include fluid mechanics and possibly fluid-structure interaction, though these are likely to be small effects and can be incorporated by adjusting the heat transfer coefficient. A simpler optimization problem is considered in the remainder of this report, which addresses these concerns.

4. Geometry Parametrization Approach

In the prior section, an integral equation approach to optimizing the barrel cross section to minimize the internal surface temperature was presented. We now adopt a parametric approach instead. It is assumed a priori that the solution will use fins. Accordingly, a simplified basic geometry parameterized to vary the fin cross sections, number of fins and tube wall thickness is used. The analysis thus provides a basis for qualitatively and quantitatively evaluating the effect of fins on the thermal and structural response of a gun tube.

4.1 Governing Equations

As stated, obtaining an analytic solution of the fully coupled transient thermostructural equations for repeated firing is only possible for simple geometries and idealized load curves. To obtain solutions for more realistic loads and geometries, a numerical solution to the governing equations is sought. The equations governing the response of the gun tube are the conservation of linear momentum equations coupled with transient heat conduction, Eqs. 34 and 35. The conservation of linear momentum in a solid is given by

$$\rho\frac{\partial^2\mathbf{u}}{\partial t^2} + \rho(\mathbf{u}\cdot\nabla)\mathbf{u} = \nabla\cdot\sigma + \mathbf{F_v}, \tag{34}$$

where ρ is the density, $\mathbf{u}$ is the displacement, σ is the Cauchy stress tensor, and $\mathbf{F_v}$ are volumetric body forces. Transient heat conduction is given by

$$\rho c_p\frac{\partial T}{\partial t} - k\nabla^2 T = q_b, \tag{35}$$

where T is the temperature, ρ is the density, c_p is the specific heat (at constant pressure), k is the thermal conductivity, and q_b are heat sources in the body. These equations can be solved numerically by various techniques.[24] In this report, the thermostructural response was modeled using the structural and heat transfer modules of COMSOL Multiphysics software suite,[11] which uses the finite element method.

Note that, from Eq. 35, the thermal diffusivity coefficient is normally defined by $\alpha = \frac{k}{\rho c_p}$.

The thermal diffusivity coefficient can be used to estimate how rapidly heat diffuses through a material. Specifically, the time required for heat to diffuse a distance r from a heat source is on the order $t = \frac{r^2}{\alpha}$. For example, a copper tube with a wall thickness of 7.62 mm has a diffusion time of 0.5 s. At a firing rate of 10 rds/s, five rounds will have been fired before the thermal wave reaches the outer boundary. For steel, a much poorer conductor, the estimated time is almost 5 s, which implies 50 rounds will have been fired before the outer wall temperature increases. Consequently, for many firing scenarios (single shot, 3-round burst), steady-state conditions are typically not attained. In fact, for sustained firing at 10 rds/s, the steady-state temperature is not reached until over 200 rounds have been fired for a steel barrel. At this point, the temperature of the inner radius may exceed 1400 °C, which is above the anneal temperature of the material.[2]

To prevent damage to the barrel, coatings on the inner barrel surface have been considered.[8] At present, using AM to add coatings is not feasible. The typical approach to reducing the steady-state temperature is to enhance the heat transfer to the surroundings by adding fins. However, as stated several times, the primary advantages of fins are only apparent once the barrel has reached a steady-state condition. The remainder of this report examines the effectiveness of fins prior to reaching steady state. Issues such as robustness of the design are not considered though they should be as the fins considered are as thin as 0.5 mm and thus susceptible to damage. Additionally, 0.5 mm is approaching the minimum printable feature size of many metal AM systems.

4.2 Parametric Analysis

To quantify the effect of using fins to manage the temperature of the barrel, a simplified geometry for the barrel with fins was created, as shown in Fig. 9. The geometric parameters allowed to vary are the outer radius, the fin width, the fin height and the number of fins, as shown in Table 2. The inner radius is fixed at 7.62 mm. Two firing rates were considered: 10 rds/s and 20 rds/s. Additionally, two values for the convective heat transfer coefficient, h_t were considered: 100 and 1000 W/(m^2 K) which are approximate values for natural convection in air, and water, respectively.

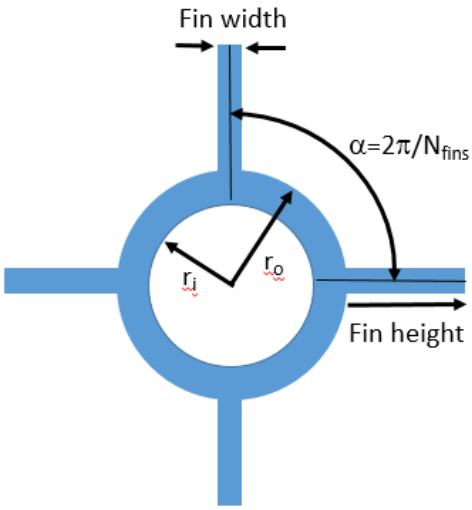

Fig. 9. Parameterized geometry

Table 2. Parameter values

Parameter	Values
Outer Radius	$\mathbf{2}\boldsymbol{r}_i$, $\mathbf{3}\boldsymbol{r}_i$
Fin width (mm)	2,**4**
Fin height (mm)	5,**10**
Number of fins	8,**4,12**
Firing rate (rds/s)	20,**10**
Convective Heat Transfer ($W/(m^2K)$)	**100, 1000**

4.3 Parametric Results

The bolded values in Table 2 are discussed in this report. The four specific fin/radii combinations examined are shown in Fig. 10. The material properties used are tabulated in Table 3. For this analysis, the steady state was assumed to be reached when the heat flux on the outer surface approached an asymptotic value. With this assumption, steady state occurred after 25 s at the 10-rds/s firing rate. The anneal temperature used for a generic steel was 1100 °C (1373 K) while the melt temperatures was 1400 °C (1673 K).

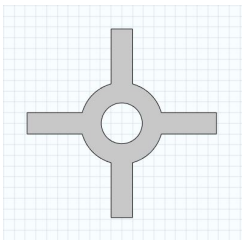

(a) 4 Fin minimum R_o

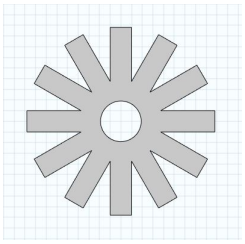

(b) 12 Fin minimum R_o

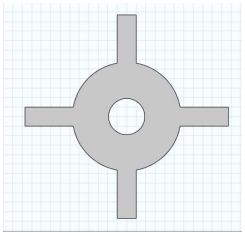

(c) 4 Fin maximum R_o

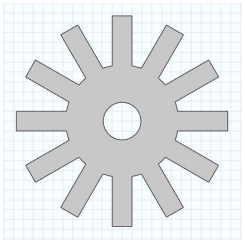

(d) 12 Fin maximum R_o

Fig. 10. Fin designs examined

Table 3. Material properties

Material Property	Copper	Steel
Thermal Conductivity ($\frac{W}{m \cdot K}$)	400	44.5
Density ($\frac{kg}{m^3}$)	8960	7850
Specific heat ($\frac{J}{kg \cdot K}$)	385	475
Thermal Diffusivity ($\frac{k}{\rho C_p}$)	1.16e-04	1.19e-05
Young's Modulus (GPa)	110	205
Yield Strength (MPa)	320	710

Figures 11a and 11b show that while fins will decrease the long-term steady-state temperature, the temperature rise is still equivalent to the temperature rise of a simple cylindrical tube. The reduction in temperature is on the order of 100 °C regardless of the number of fins. The maximum temperature is always at the inner surface as expected. The saw-tooth pattern of the response is due to sampling aliasing of the input temperature cycling curve, (Fig. 1). If the temperature had been sampled at a higher rate, this pattern would resemble that input curve. Despite this sampling issue, the overall conclusions regarding the temperature rise in the barrel still hold.

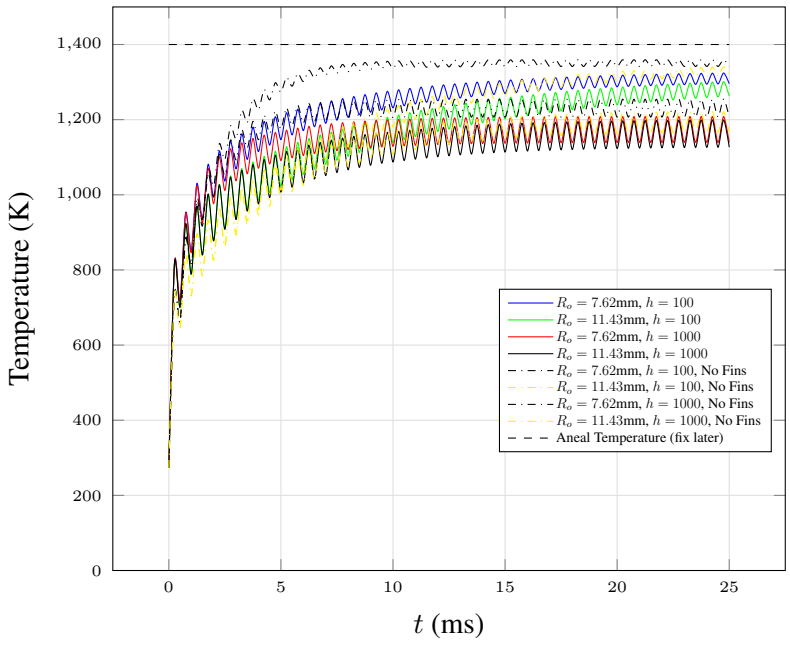

(a) Maximum Temperature (4 fins)
($\mathrm{Fin}_{\mathrm{height}}$**=10mm,**$\mathrm{Fin}_{\mathrm{width}}$**=4mm)**

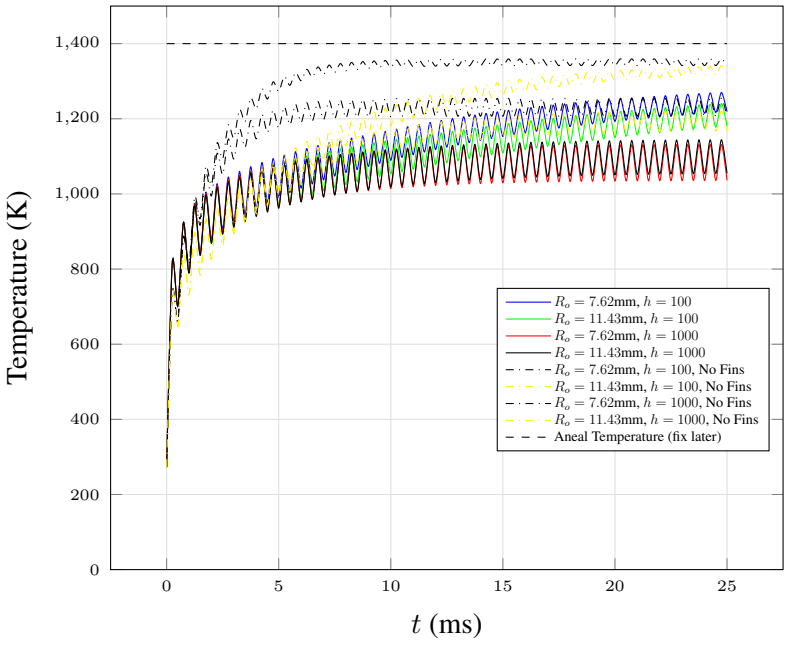

(b) Maximum Temperature (12 fins)
($\mathrm{Fin}_{\mathrm{height}}$**=10mm,**$\mathrm{Fin}_{\mathrm{width}}$**=4mm)**

Fig. 11. Maximum Temperature due to repeated fire

Finally, maximum von Mises stress profiles are shown in Fig. 12. It is observed that the maximum stress is either at the inner surface or near the base of the fins. The high values due to the fins could be mitigated by simply including fillets where they meet the tube. Therefore, these stresses can be safely ignored. The von Mises stress profiles with the heat transfer coefficient $h = 1000$ W/(m^2 K) are similar. The analysis indicates that maximum von Mises stress is on the order of 1 GPa. Therefore, it is not expected that the tube will fail due to overstress as hardened steels can sustain stresses in excess of 2 GPa.

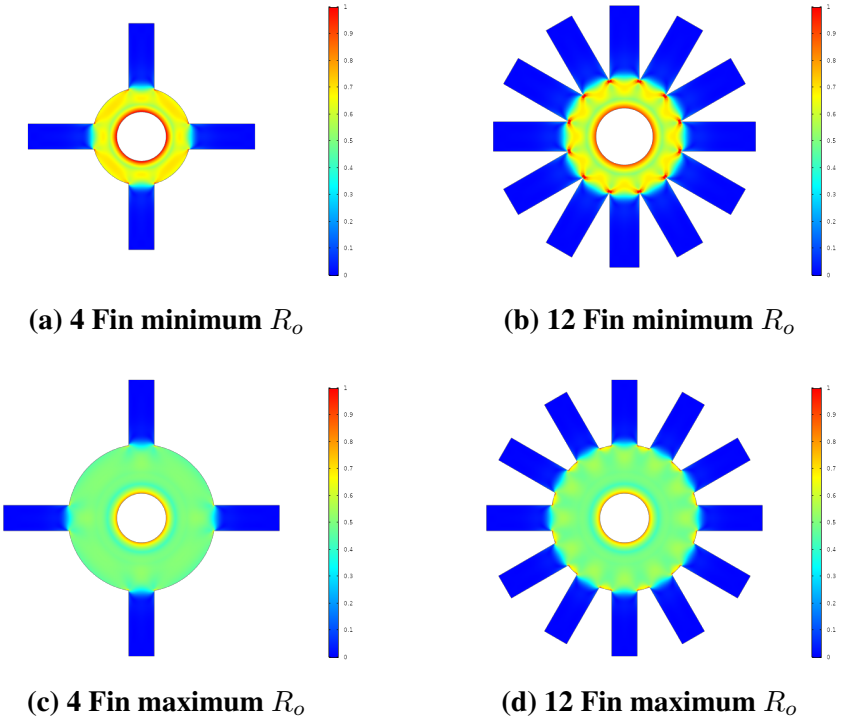

(a) 4 Fin minimum R_o **(b) 12 Fin minimum R_o**

(c) 4 Fin maximum R_o **(d) 12 Fin maximum R_o**

Fig. 12. von Mises stress comparison with heat flux coefficient of 100

5. Conclusions

Two method were implemented to explore the effect of gun tube geometry on thermal and mechanical performance. One method used a boundary integral approach. The other used a parametric fin design with a finite element method. AM could likely facilitate the fabrication of these designs.

It was found that while the addition of fins to the gun tube geometry may help with steady-state temperature, transient effects dominate and finned designs cannot com-

pensate for the lag in temperature increase due to diffusivity. Therefore, from the viewpoint of optimizing the heat transfer from a gun tube, it is not obvious that designs incorporating fins for passive cooling offer much improvement over the traditional simple cylinder design. Consequently, a conclusion noted more than 40 years prior,[2] "Heavy tubes or light tubes with cooling fins will reach steady state later than plain light tubes. If the yield strength at steady state temperature approaches the firing stresses, continued firing becomes dangerous", is still appropriate today.

However, there are other approaches for enhancing heat transfer from cylindrical tubes,[21] such as using bi-material or graded material construction, which the use of AM may make more feasible.

6. References

1. NIST Advanced Manufacturing Series 100-16. Literature review of metal additive manufacturing defects. Washington (DC): National Institute of Standards and Technology; 2018.

2. AMCP 706-252. Research and development of material, engineering design handbook, guns series, gun tubes. Washington (DC): Army Material Command (US); 1964.

3. Taylor G. Strains in a gun barrel near the driving barrel of a moving projectile. London (UK): UK Ministry of Supply; 1942 March. Report No.: A.C. 1851/Gn.

4. Simkins T. Resonance of flexural waves in gun tubesl. Watervliet (NY): Benet Weapons Laboratory; 1987 July. Report No.: ARCCB-TR-87008.

5. Montgomery J, Ellis R. Large caliber gun tube materials systems design. In: 10th US Army Gun Dynamics Symposium Proceedings; 2001 Apr 23–26; Austin, TX. p. 385–397.

6. Bannister E, Jones R, D.W. B. Heat transfer, barrel temperatures and thermal strains in guns. Aberdeen Proving Ground (MD): Ballistic Research Laboratory (US); 1963 Feb. Report No.: Report No. 1192.

7. Babaei H, Malakzadeh M, Asgari H. Stress analysis of gun barrel subjected to dynamic pressure. Int Mech Eng and Appl. 2015;3(4):71–80.

8. Conroy P, P. W, M.J. N. Gun tube coatings in distress. Aberdeen Proving Ground (MD): Army Research Laboratory (US); 2001 Feb. Report No.: ARL-TR-2393.

9. Timoshenko S, Goodier J. Theory of elasticity. 2d ed. New York: McGraw-Hill Book Company; 1951.

10. Kandil A. Analysis of thick-walled cylindrical pressure vessels under the influence of cyclic internal pressure and cyclic temperature. Int J Mech Sci. 1996;38(12):1319–1332.

11. COMSOL, Inc. COMSOL Multiphysics reference manual, version 5.3. 2018.

12. Smith M. Abaqus/standard user's manual, version 6.9. Providence (RI): Simulia; 2009.

13. DeSalvo GJ, Swanson JA. Theory reference for the mechanical apdl and mechanical applications. Houston (Pa): Swanson Analysis Systems; 2009.

14. Wilkerson S, Hopkins D. Analysis of a balanced breech system for the m1a1 main gun system using finite element techniques. Aberdeen Proving Ground (MD): Army Research Laboratory (US); 1994 Nov. Report No.: ARL-TR-608.

15. Gough PS. The xnovaktc code. Aberdeen Proving Ground (MD): Ballistic Research Laboratory (US); 1990 Feb. Report No.: BRL-CR-627.

16. Gough P. Interior ballistics modeling: Extensions to the one-dimensional xktc code and analytical studies of pressure gradient for lumped parameter codes. Aberdeen Proving Ground (MD): Army Research Laboratory (US); 2001 Feb. Report No.: ARL-CR-460.

17. Moeller C. Measurement of transient bore-surface temperatures in 7.62 mm gun tubes. Rock Island Arsenal (IL): Midwest Research Institute; 1973 Nov. Report No.: AD-780 938.

18. Banerjee P, Butterfield R. Boundary element methods in engineering science. London (UK): McGraw-Hill Book Co.; 1981.

19. Beer G. Programming the boundary element method. Baffins Lane, Chichester, West Sussex (UK): John Wiley and Sons, Ltd; 2001.

20. Canino LF, Ottusch JJ, Stalzer MA, Visher JL, Wandzura SM. Numerical solution of the Helmholtz equation in 2-D and 3-D using a high-order Nyström discretization. Journal of Computational Physics. 1998;146(2):627–663.

21. Özişik MN. Heat transfer, a basic approach. New York: McGraw-Hill Publishing Co.; 1985.

22. Behrou R, Guest JK. Topology optimization for transient response of structures subjected to dynamic loads. In: 18th AIAA/ISSMO Multidisciplinary Analysis and Optimization Conference; 2017 June 5-9; Denver, CO. p. 3657.

23. Mrzygłód MW, Duda P. Topology optimization of structures subjected to transient thermomechanical loading. In: 1st Renewable Energy Sources-Research and Business (RESRB-2016); 2016 June 22–24; Wrocław, Poland. p. 383–388.

24. Hughes TJR. The finite element method, linear static and dynamic finite element analysis. Englewood Cliffs (NJ): Prentice-Hall, Inc.; 1987.

1 (PDF) DEFENSE TECHNICAL INFORMATION CTR
DTIC OCA

1 (PDF) FCDD RLD CL
TECH LIB

42 (PDF) DIR CCDC ARL
FCDD RLD
H MAUPIN
M TSCHOPP
FCDD RLW
S KARNA
A RAWLETT
S SCHOENFELD
J SOUTH
FCDD RLW L
O OBERLE
FCDD RLW LB
B BARNES
E BYRD
J LARENTZOS
R PESCE-RODRIGUEZ
B RICE
C WU
FCDD RLW LD
P CONROY
M NUSCA
J SCHMIDT
FCDD RLW M
B LOVE
FCDD RLW MA
J LASCALA
D O'BRIEN
FCDD RLW MB
B AKSOYLU
C FOUNTZOULAS
A GAYNOR
G GAZONAS
E HERNANDEZ
D HOPKINS
R WILDMAN
FCDD RLW MD
K CHO
M PEPI
FCDD RLW ME
M GOLT
J LASALVIA
S SILTON
FCDD RLW MF
K DARLING
R DOWDING
A GIRI
P GOINS
C HAINES
FCDD RLW MG
J ANDZELM
J LENHART
B RINDERSPACHER
J ROBINETTE
T SIRK
FCDD RLW S
J CIEZAK–JENKINS

4 (PDF) COMMANDER CCDC AC
FCDD ACM EP
C ADAM
E CARAVACA
K CHI
C HOUTHUYSEN

4 (PDF) NSWC
ENERGETIC SYS DIV SURF WEAPON
ENG BR
M BONANNO
E TERSINE
IH EODTD MD
A IHNEN